

Vibrational density of states of jammed packing at high dimensions: mean-field theory

Harukuni Ikeda*

Department of Physics, Gakushuin University, 1-5-1 Mejiro, Toshima-ku, Tokyo 171-8588, Japan

Masanari Shimada

Department of Physics, Toronto Metropolitan University, M5B 2K3, Toronto, Canada

(Dated: June 28, 2022)

Several mean-field theories predict that the Hessian matrix of amorphous solids converges the Wishart matrix in the limit of the large spatial dimensions $d \rightarrow \infty$. Motivated by these results, we here calculate the density of states of random packing of harmonic spheres by mapping the Hessian of the original system to the Wishart matrix. We compare our result with that of previous numerical simulations of harmonic spheres in several spatial dimensions $d = 3, 5, \text{ and } 9$. For small pressure $p \ll 1$ (near jamming), we find a good agreement even in $d = 3$, and obtain better agreements in larger d , suggesting that the approximation becomes exact in the limit $d \rightarrow \infty$.

I. INTRODUCTION

The vibrational density of states $D(\omega)$ plays a central role to characterize the low-temperature properties of solids. For both crystals and amorphous solids, $D(\omega)$ for small ω eventually follows the prediction of the Debye model $D(\omega) \sim \omega^{d-1}$, suggesting that the vibrational excitation is dominated by phonon modes [1, 2]. However, for amorphous solids, in addition to the phonon modes, there arise excess non-phonon modes for small ω . This phenomenon, often referred to as the boson peak, is considered as a universal feature of amorphous solids [3].

From the theoretical point of view, a first step to tackle the problem is to consider mean-field models/theories. Several mean-field models, such as the p -spin spherical model [4] and perceptron [5], and theories, such as the effective medium theory [6, 7], cavity method [8], etc. [9–12], suggest that Hessian matrices of amorphous solids are approximated by the Wishart matrix. However, somewhat surprisingly, the functional form of $D(\omega)$ of particle systems has not been calculated yet, even in the large dimensional limit $d \rightarrow \infty$, where the mean-field theory becomes exact. As a consequence, one should introduce fitting parameters to compare the theory and numerical results [9, 11, 13], even in large d [14].

In this work, we focus on frictionless spherical particles interacting with the harmonic potential [15]. Since the harmonic potential is a purely repulsive potential, the system gets unstable in the zero pressure limit $p \rightarrow 0$, which is known as the (un)jamming transition [15]. Near the jamming transition point ($p \ll 1$), several physical quantities, such as the contact number z , exhibit the power-law behavior [15]. The critical exponents near the jamming transition are calculated by several mean-field theories [6, 16–18]. However, again, the detailed functional form of z is still undetermined, even in $d \rightarrow \infty$.

Recently, one of the present authors performed an extensive numerical simulation of harmonic spheres and cal-

culated $D(\omega)$ and z in spatial dimensions from $d = 3$ to $d = 9$ [19]. Therefore, it is now desirable to directly compare the numerical results in large d with the predictions of the mean-field theory.

Here, we theoretically calculate $D(\omega)$ and z of harmonic spheres in large d , and compare them with the previous numerical results. For this purpose, inspired by the previous mean-field calculations, we assume that the Hessian of harmonic spheres converges to the (shifted) Wishart matrix in the mean-field limit $d \rightarrow \infty$. We determine the pre-factors of the Wishart matrix so that its trace is consistent with that of the Hessian of the original model. For small pressure, our results well agree with the previous numerical results [19] even in $d = 3$, and obtain better agreements in larger d , suggesting that our theory becomes exact in the limit of $d \rightarrow \infty$.

The organization of the paper is as follows. In Sec. II, we introduce the model and several physical quantities. In Sec. III, we calculate $D(\omega)$ in the limit of $d \rightarrow \infty$. In Sec. IV, we summarize the results.

II. SETTINGS

Here we introduce the model and several physical quantities. We consider a system consisting of frictionless spherical particles interacting with the harmonic potential [15]:

$$V = \sum_{i < j}^{1, N} k \frac{h_{ij}^2}{2} \theta(-h_{ij}), \quad h_{ij} = |\mathbf{r}_i - \mathbf{r}_j| - R_i - R_j \quad (1)$$

where N denotes the number of particles, k denotes the spring constant, and $\theta(x)$ denotes the Heaviside step function. $\mathbf{r}_i = \{x_{i1}, \dots, x_{id}\}$ and R_i denote the position and radius of the i -th particle, respectively. To simplify the notation, hereafter, we set $k = 1$.

* harukuni.iked@gakushuin.ac.jp

The Hessian of the potential is

$$\begin{aligned}\mathcal{H}_{ia,jb} &= \frac{\partial^2 V}{\partial x_{ia} \partial x_{jb}} = \mathcal{H}_{ia,jb}^{(1)} + \mathcal{H}_{ia,jb}^{(2)}, \\ \mathcal{H}_{ia,jb}^{(1)} &= \sum_{\mu=1}^{Nz/2} \frac{\partial h_{\mu}}{\partial x_{ia}} \frac{\partial h_{\mu}}{\partial x_{jb}}, \quad \mathcal{H}_{ia,jb}^{(2)} = \sum_{\mu=1}^{Nz/2} h_{\mu} \frac{\partial^2 h_{\mu}}{\partial x_{ia} \partial x_{jb}},\end{aligned}\quad (2)$$

where

$$z = \frac{1}{N} \sum_{i < j} \theta(-h_{ij}). \quad (3)$$

denotes the number of contacts per particle, and $\sum_{\mu=1}^{Nz/2}$ denotes the sum of all pairs $\mu = (ij)$ for which $h_{ij} < 0$. Once we have the eigenvalue distribution of \mathcal{H} , $\rho(\lambda)$, the vibrational density of states $D(\omega)$ is calculated as

$$D(\omega) = 2\omega\rho(\lambda = \omega^2). \quad (4)$$

For the control parameter, we use the *pre-stress* defined as [19]

$$e = -\frac{2(d-1)}{Nz} \sum_{\mu=1}^{Nz/2} \frac{h_{\mu}}{r_{\mu}} = (d-1) \left\langle \frac{R_i + R_j}{r_{ij}} - 1 \right\rangle, \quad (5)$$

where $\langle \bullet \rangle$ denotes the average for the all contacts $\langle \bullet \rangle = (Nz/2)^{-1} \sum_{i < j} \theta(-h_{ij}) \bullet$. The right most expression in Eq. (5) clearly shows that e is proportional to the average overlap of particles. The proportional constant $(d-1)$ has been chosen so that e remains finite in the limit $d \rightarrow \infty$ [19]. Near the jamming transition point, e is proportional to the pressure, $e \sim p$ and vanishes at the jamming transition point. In a previous numerical study [14], the packing fraction was used as a control parameter. However, it has been pointed out that e is a more natural control parameter [19, 20]. Below, we calculate z and $D(\omega)$ as functions of e .

III. THEORY

A. Summary of previous works

Here we briefly review the previous works. The seminal work has been done by G. Parisi [8]. He showed that the eigenvalue distribution of the Hessian of harmonic spheres converges to the Marcenko-Pastur distribution in the limit $d \rightarrow \infty$, meaning that the Hessian is identified with the Wishart matrix $\mathcal{H} \sim \mathcal{W}$ [8], but the effects of the pre-stress e were neglected at that time. More recently, G. Parisi with coauthors performed a more complete analysis for the perceptron, which is a mean-field model of random sphere packing of harmonic spheres [17, 21]. The analysis of the perceptron suggests

that the Hessian of harmonic spheres in large d is written as

$$\mathcal{H}_{\text{MF}} = a\mathcal{W} + be\mathcal{I}, \quad (6)$$

where a and b denote constants, $\mathcal{I}_{ia,jb} = \delta_{ia,jb}$ denotes the identity matrix, and

$$\mathcal{W}_{ia,jb} = \frac{2}{Nz} \sum_{\mu=1}^{Nz/2} \xi_{ia}^{\mu} \xi_{jb}^{\mu} \quad (7)$$

denotes the Wishart matrix. ξ_{ia}^{μ} denotes the i.i.d gaussian random variable with zero mean and unit variance [5]. The replica calculation of the perceptron also proves the marginal stability [22]: the minimal eigenvalue λ_{\min} of the Hessian \mathcal{H} vanishes $\lambda_{\min} = 0$ near the jamming transition point [5]. Interestingly, several other mean-field theories also suggest that the Hessian of harmonic spheres is written as Eq. (6), though the precise values of a and b are still unknown [6, 9–11, 23].

In this work, we use Eq. (6) as an Ansatz. We determine a and b by requiring that the trace of \mathcal{H}_{MF} is consistent with that of the Hessian of the original model, Eq. (2).

B. Calculation of a and b

For simplicity, we first discuss the case without pre-stress. By setting $e = 0$, we get

$$\mathcal{H} \rightarrow \mathcal{H}^{(1)}, \quad \mathcal{H}_{\text{MF}} \rightarrow a\mathcal{W}. \quad (8)$$

Then, we determine a from the following condition:

$$\text{Tr}\mathcal{H}^{(1)} = a\text{Tr}\mathcal{W}. \quad (9)$$

The LHS in Eq. (9) can be calculated as

$$\text{Tr}\mathcal{H}^{(1)} = \sum_{i=1}^N \sum_{a=1}^d \sum_{\mu=1}^{Nz/2} \left(\frac{\partial h_{\mu}}{\partial x_{ia}} \right)^2 = Nz, \quad (10)$$

where we used

$$\frac{\partial h_{ij}}{\partial x_{ka}} = (\delta_{ik} - \delta_{jk}) \frac{x_{ia} - x_{ja}}{|\mathbf{r}_i - \mathbf{r}_j|}, \quad \sum_{k=1}^d \sum_{a=1}^d \left(\frac{\partial h_{ij}}{\partial x_{ka}} \right)^2 = 2. \quad (11)$$

The RHS is

$$a\text{Tr}\mathcal{W} = \frac{2a}{Nz} \sum_{i=1}^N \sum_{a=1}^d \sum_{\mu=1}^{Nz/2} (\xi_{ia}^{\mu})^2 = aNd. \quad (12)$$

By using Eqs. (9), (10) and (12), we get

$$a = \frac{z}{d}. \quad (13)$$

Next we consider the full matrix including the term proportional to e . Assuming that $\text{Tr}\mathcal{H} = \text{Tr}\mathcal{H}_{\text{MF}}$, we get

$$\begin{aligned} \text{Tr} \left(\mathcal{H}^{(1)} + \mathcal{H}^{(2)} \right) &= \text{Tr} (a\mathcal{W} + be\mathcal{I}) \\ \rightarrow \text{Tr}\mathcal{H}^{(2)} &= be\text{Tr}\mathcal{I}. \end{aligned} \quad (14)$$

The LHS can be calculated as

$$\begin{aligned} \text{Tr}\mathcal{H}^{(2)} &= \sum_{i=1}^N \sum_{a=1}^d \sum_{\mu=1}^{Nz/2} h_{\mu} \frac{\partial^2 h_{\mu}}{\partial x_{ia}^2} \\ &= 2(d-1) \sum_{\mu=1}^{Nz/2} \frac{h_{\mu}}{r_{\mu}} \\ &= -Nze, \end{aligned} \quad (15)$$

where we used

$$\begin{aligned} \frac{\partial^2 h_{ij}}{\partial x_{ka}^2} &= (\delta_{ik} + \delta_{jk}) \frac{r_{ij}^2 - (x_{ia} - x_{jb})^2}{r_{ij}^3}, \\ \sum_{k=1}^N \sum_{a=1}^d \frac{\partial^2 h_{ij}}{\partial x_{ka}^2} &= 2 \frac{d-1}{r_{ij}}. \end{aligned} \quad (16)$$

From Eqs. (14), (15) and $\text{Tr}\mathcal{I} = Nd$, we get

$$b = -\frac{z}{d}. \quad (17)$$

In summary, we get

$$\mathcal{H}_{\text{MF}} = \frac{z}{d}\mathcal{W} - \frac{z}{d}e\mathcal{I}. \quad (18)$$

C. Eigenvalue distribution

It is well-known that the eigenvalue distribution of the Wishart matrix \mathcal{W} follows the Marchenko-Pastur law [24]

$$\rho_{\text{MP}}(\lambda) = \frac{z}{2d} \frac{\sqrt{(\lambda_+ - \lambda)(\lambda - \lambda_-)}}{2\pi\lambda}, \quad \lambda_{\pm} = \left(1 \pm \sqrt{\frac{2d}{z}} \right)^2. \quad (19)$$

Let \mathbf{e}_n be an eigenvector of \mathcal{W} , and λ_n^{MP} be the corresponding eigenvalue. Then, we have

$$\mathcal{H}_{\text{MF}} \cdot \mathbf{e}_n = \left(\frac{z}{d}\lambda_n^{\text{MP}} - \frac{z}{d}e \right) \mathbf{e}_n, \quad (20)$$

meaning that \mathbf{e}_n is also an eigenvector of \mathcal{H}_{MF} and the corresponding eigenvalue is $\lambda_n = \frac{z}{d}\lambda_n^{\text{MP}} - \frac{z}{d}e$. Therefore, the eigenvalue distribution of \mathcal{H}_{MF} is calculated as

$$\rho(\lambda) = \rho_{\text{MP}}(\lambda_{\text{MP}}) \frac{d\lambda_{\text{MP}}}{d\lambda} = \frac{d}{z} \rho_{\text{MP}}(d\lambda/z + e). \quad (21)$$

In particular, the minimal eigenvalue is

$$\lambda_{\min} = \frac{z}{d} \left(1 - \sqrt{\frac{2d}{z}} \right)^2 - \frac{z}{d}e. \quad (22)$$

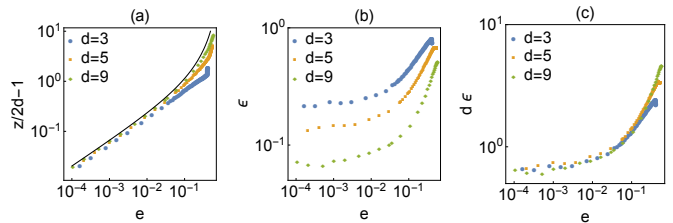


FIG. 1. (a) e dependence of z . Markers denote numerical results taken from Ref. [19], while the solid line denotes the theoretical prediction. (b) ϵ for the same data. (c) $d\epsilon$ for the same data.

D. Marginal stability and contact number

The replica calculation in the limit $d \rightarrow \infty$ predicts that the system is marginally stable near the jamming transition point, $\lambda_{\min} = 0$ [25] [5, 18, 26]. By using the marginal stability and Eq. (22), we get

$$\frac{z(e)}{2d} = \frac{1}{(1 - e^{1/2})^2}. \quad (23)$$

Here we assumed that z/d takes a finite value in the limit $d \rightarrow \infty$, because the numerical results suggest that $z \rightarrow 2d$ at the jamming transition point [15]. For $e \ll 1$, we reproduce the well-known scaling observed by numerical simulations [15]

$$z/2d - 1 \sim 2e^{1/2} \sim p^{1/2}. \quad (24)$$

The critical exponent 1/2 was previously derived by using the variational argument [16], effective medium theory [6], and replica theory [17], but our result Eq. (23) also allows us to access the pre-factor and non-linear terms. Somewhat surprisingly, Eq. (23) suggests that $z(e)$ depends only on e , and does not depend on the preparation protocols. It is interesting future work to see if this property survives in finite d .

In Fig. 1 (a), we compare Eq. (23) with numerical results in several spatial dimensions d obtained by rapid quench from high temperature random configurations. See Ref. [19] for the details of the numerical simulations. The theory well agrees with the numerical results for small e . For more quantitative discussion, in Fig. 1 (b), we show the difference between the results of the theory z_{the} and simulation z_{sim} :

$$\epsilon = \frac{z_{\text{the}}/2d - 1 - (z_{\text{sim}}/2d - 1)}{z_{\text{the}}/2d - 1} = \frac{z_{\text{the}} - z_{\text{sim}}}{z_{\text{the}} - 2d}. \quad (25)$$

The data collapse onto a single curve if we rescale the vertical axis by d (Fig. 1 (c)), meaning that the deviation scales as $\epsilon \sim 1/d$.

E. Vibrational density of states

By using Eq. (21), the vibrational density of states $D(\omega)$ is calculated as $D(\omega) = 2\omega\rho(\lambda = \omega^2)$. Although

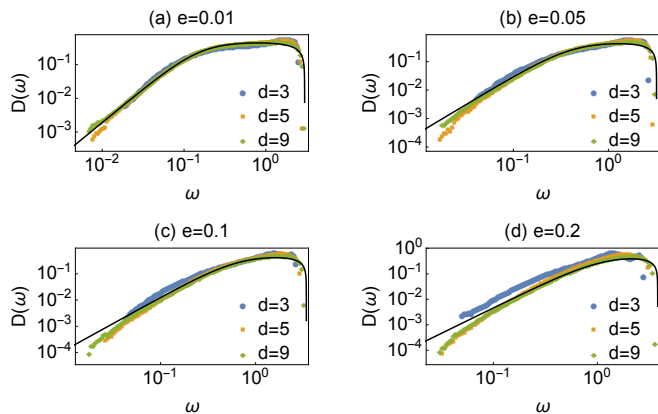


FIG. 2. Density of states $D(\omega)$. Markers denote numerical results taken from Ref. [19]. The solid lines denote theoretical predictions.

$D(\omega)$ depends on both z and e , Eq. (23) allows us to eliminate the dependency on z . After some manipulations, we get

$$D(\omega) = \frac{\omega^2 \sqrt{(1 - e^{1/2})^3 \{8 - (1 - e^{1/2})\omega^2\}}}{2\pi \{2e + (1 - e^{1/2})^2\omega^2\}}. \quad (26)$$

In Fig. 2, we compare the theoretical prediction Eq. (26) and numerical results. The results are consistent near jamming $e = 0.01$ even in $d = 3$, while there is a visible deviation for small ω far from jamming $e = 0.2$ even in $d = 9$. It is an interesting future work to see if a better agreement is obtained in higher d .

For $e \ll 1$ and $\omega \ll 1$, we get the following scaling:

$$D(\omega) \sim \frac{\omega^2 \sqrt{\omega_{\max}^2 - \omega^2}}{2\pi(\omega^2 + \omega_*^2)} \sim \begin{cases} \text{const} & \omega \gg \omega_* \\ \delta z^{-2} \omega^2 & \omega \ll \omega_*, \end{cases} \quad (27)$$

where $\omega_{\max} = 2\sqrt{2}$, and $\omega_* = \sqrt{2}e \propto z/2d - 1$. In particular, $D(\omega) = \text{const}$ at the jamming transition point $e = 0$. The similar results have been previously derived by applying the effective medium theory to the disordered lattices [6], and the replica method to the mean-field models [5, 23].

IV. SUMMARY

In this work, we calculated the contact number z and vibrational density of states $D(\omega)$ for harmonic spheres in the large spatial dimensions $d \rightarrow \infty$. Our theoretical results well agree with the results of the previous numerical simulation in large d .

Our theoretical results are relied on the Ansatz Eq. (6), that is, the Hessian of harmonic spheres has the form of the shifted Wishart matrix. The consistency between our theoretical results and previous numerical results suggests that the Ansatz becomes exact in the limit $d \rightarrow \infty$. This result motivates us to develop more rigorous calculation in $d \rightarrow \infty$ without using the Ansatz, as done in the previous exact calculations for hard spheres [26–28]. We left it as future work.

ACKNOWLEDGMENTS

We thank F. Zamponi for useful comments. This project has received JSPS KAKENHI Grant Numbers 21K20355 and 19J20036.

-
- [1] C. Kittel and P. McEuen, *Introduction to solid state physics*, Vol. 8 (Wiley New York, 1976).
 - [2] H. Mizuno, H. Shiba, and A. Ikeda, Proceedings of the National Academy of Sciences **114**, E9767 (2017).
 - [3] W. A. Phillips and A. Anderson, *Amorphous solids: low-temperature properties*, Vol. 24 (Springer, 1981).
 - [4] G. Biroli and J.-P. Bouchaud, Structural Glasses and Supercooled Liquids: Theory, Experiment, and Applications, 31 (2012).
 - [5] S. Franz, G. Parisi, P. Urbani, and F. Zamponi, Proceedings of the National Academy of Sciences **112**, 14539 (2015).
 - [6] E. DeGiuli, A. Laversanne-Finot, G. Düring, E. Lerner, and M. Wyart, Soft Matter **10**, 5628 (2014).
 - [7] M. Shimada and E. De Giuli, arXiv preprint arXiv:2008.11896 (2020).
 - [8] G. Parisi, arXiv preprint arXiv:1401.4413 (2014).
 - [9] Y. Beltukov, JETP Letters **101**, 345 (2015).
 - [10] G. M. Cicuta, J. Krausser, R. Milkus, and A. Zaccone, Phys. Rev. E **97**, 032113 (2018).
 - [11] M. Baggioli, R. Milkus, and A. Zaccone, Phys. Rev. E **100**, 062131 (2019).
 - [12] M. Baggioli and A. Zaccone, Phys. Rev. Research **1**, 012010 (2019).
 - [13] M. L. Manning and A. J. Liu, EPL (Europhysics Letters) **109**, 36002 (2015).
 - [14] P. Charbonneau, E. I. Corwin, G. Parisi, A. Poncet, and F. Zamponi, Phys. Rev. Lett. **117**, 045503 (2016).
 - [15] C. S. O’Hern, L. E. Silbert, A. J. Liu, and S. R. Nagel, Phys. Rev. E **68**, 011306 (2003).
 - [16] M. Wyart, L. E. Silbert, S. R. Nagel, and T. A. Witten, Phys. Rev. E **72**, 051306 (2005).
 - [17] S. Franz, G. Parisi, M. Sevelev, P. Urbani, and F. Zamponi, (2017).
 - [18] G. Parisi, P. Urbani, and F. Zamponi, *Theory of simple glasses: exact solutions in infinite dimensions* (Cambridge University Press, 2020).

- [19] M. Shimada, H. Mizuno, L. Berthier, and A. Ikeda, *Physical Review E* **101**, 052906 (2020).
- [20] D. Bi, S. Henkes, K. E. Daniels, and B. Chakraborty, *Annu. Rev. Condens. Matter Phys.* **6**, 63 (2015).
- [21] S. Franz and G. Parisi, *Journal of Physics A: Mathematical and Theoretical* **49**, 145001 (2016).
- [22] M. Müller and M. Wyart, (2015).
- [23] H. Ikeda, *Phys. Rev. Research* **2**, 033220 (2020).
- [24] G. Livan, M. Novaes, and P. Vivo, *Introduction to random matrices: theory and practice*, Vol. 26 (Springer, 2018).
- [25] Here we take the limit $d \rightarrow \infty$ so that z/d remains finite. This is consistent with the numerical result the jamming transition point where $z \approx 2d$ [15].
- [26] J. Kurchan, G. Parisi, P. Urbani, and F. Zamponi, *The Journal of Physical Chemistry B* **117**, 12979 (2013).
- [27] J. Kurchan, G. Parisi, and F. Zamponi, *Journal of Statistical Mechanics: Theory and Experiment* **2012**, P10012 (2012).
- [28] P. Charbonneau, J. Kurchan, G. Parisi, P. Urbani, and F. Zamponi, *Journal of Statistical Mechanics: Theory and Experiment* **2014**, P10009 (2014).